# Magnetic exchange interactions in B-, Si-, and As-doped $Fe_2P$ from first-principles theory

E. K. Delczeg-Czirjak,[1,*] Z. Gercsi,[2] L. Bergqvist,[1] O. Eriksson,[3] L. Szunyogh,[4] P. Nordblad,[5] B. Johansson,[1,3] and L. Vitos[1,3,6]

[1]*Applied Materials Physics, Department of Materials Science and Engineering, Royal Institute of Technology (KTH), SE-100 44 Stockholm, Sweden*

[2]*Department of Physics, Blackett Laboratory, Imperial College London, London SW7 2AZ, United Kingdom*

[3]*Department of Physics and Astronomy, Uppsala University, Box 516, 751 20 Uppsala, Sweden*

[4]*Department of Theoretical Physics and Condensed Matter Research Group of the Hungarian Academy of Sciences, Budapest University of Technology and Economics, Budafoki út 8, H-1111 Budapest, Hungary*

[5]*Department of Engineering Sciences, Uppsala University, Box 534, SE-751 21 Uppsala, Sweden*

[6]*Research Institute for Solid State Physics and Optics, P.O. Box 49, H-1525 Budapest, Hungary*

(Received 2 March 2012; revised manuscript received 28 April 2012; published 28 June 2012)

Di-iron phosphide ($Fe_2P$) is a parent system for a set of magnetocaloric materials. Although the magnetic ordering temperature ($T_C = 215$ K) of the stoichiometric composition is too low for room-temperature magnetic refrigeration, the partial replacement of P with B, Si, or As elements results in a steep increase in the magnetic ordering temperature. Doping leads to different equilibrium volumes and hexagonal axial ratios ($c/a$) within the same crystallographic phase over a wide concentration range. Here, using first principles theory, we decompose the change in the total magnetic exchange interaction upon doping into chemical and structural contributions, the latter including the $c/a$-ratio and volume effects. We demonstrate that for the investigated alloys the structural effect can be ascribed mainly to the decrease in the $c/a$ ratio that strengthens the magnetic exchange interactions between the two Fe sublattices.

DOI: 10.1103/PhysRevB.85.224435 PACS number(s): 75.30.Et, 75.30.Sg, 71.20.Be, 75.50.Bb

## I. INTRODUCTION

Di-iron phosphide ($Fe_2P$) is a prototype compound for a family of promising magnetocaloric materials,[1–6] obtained by partial substitution of Fe and P. $Fe_2P$ shows a sharp first-order-type transition from a paramagnetic (PM) to a ferromagnetic (FM) state around 215 K.[7,8] Magnetic and crystallographic properties of alloys obtained by substitution on the Fe site have been discussed from experimental[9–13] and theoretical points of view.[14] They show either ferromagnetism with a slightly increased Curie temperature[9–11] or antiferromagnetism.[9,12,13] The partial replacement of P by B[15], Si[16] or As[17] manifests into a steep increase of the magnetic transition temperature (see Fig. 1 after Refs. 15–17). About 8 at% of B doping results in a doubled magnetic transition temperature. The effect of Si is also significant: 10 at% Si addition leads to a 60% increase in $T_C$ with an almost-linear change up to 35 at% Si. In the case of As, the $T_C$ versus composition curve has the smallest slope, is nonlinear, and shows a saturation at 40 at% As, where $T_C$ reaches its maximum of 470 K.

The strong sensitivity of the Curie temperature of $Fe_2P$ was discussed by Lundgren *et al.*[18] in the context of the presence of Fe vacancy, stress, and pressure. They showed that $T_C$ correlates with the change in lattice parameters. The anomalous cell axis behavior and its correlation with $T_C$ were found in the case of Si doping.[16] A strong magnetostructural coupling was pointed out for the $(MnFe)_{1.95}P_{0.5}Si_{0.5}$ compound in Ref. 19.

On the theoretical side, $Fe_2P$ was analyzed early on by Wohlfart[20] and Moriya and Usami.[21] They proposed an itinerant electron description for systems which do not obey Hund's rules. This conclusion was corroborated by first principles theory, which reproduced the magnetic moments with an acceptable agreement.[22–25] The sharp first-order-type magnetic phase transition was attributed to the metamagnetic behavior of one of the Fe sublattices of $Fe_2P$, discussed by means of the Landau phenomenological theory.[26] Our previous study on the structural stability of Si doped $Fe_2P$[27] showed that the total energy difference between the FM and the PM phases calculated at a fixed crystal structure as a function of Si content leads to about a 3.3% increase in $T_C$ upon 10 at% Si doping, which is much lower than the experimental finding. This result indicates that a model that takes into account only the composition change is not adequate to describe the composition dependence of the Curie temperature of $Fe_2P$-based systems. A strong relation between the magnetic behavior and the structure was observed recently for MnP-related *Pnma* compounds.[28] It was reported that the magnetic ground state strongly depends on the intralayer Mn-Mn separation.

The above experimental and theoretical findings motivated us to investigate the effect of chemical and structural changes in $Fe_2P_{1-x}T_x$ ($x < 15\%$ for B, $x \leqslant 25\%$ for Si, and $x \leqslant 65\%$ for As) alloys. We study the magnetic properties of pure and doped systems by monitoring the magnetic exchange interactions ($J_{ij}$) as a function of volume, hexagonal axial ratio ($c/a$), and doping elements. We show that besides the obvious chemical effect, the structural effect turns out to be crucial when tracing the compositional changes in the magnetic properties. We find that, to a very good approximation, the structural effect may be represented by the change in the $c/a$ ratio.

The article is organized as follows: Section II gives a short description of the crystal structure, the applied *ab initio* method, and the numerical details. The results are presented and discussed in Secs. III and IV, respectively. Section V contains the main conclusions.

## II. CRYSTAL STRUCTURE AND NUMERICAL DETAILS

The $Fe_2P_{1-x}T_x$ ($x < 15\%$ for B, $x \leqslant 25\%$ for Si, and $x \leqslant 65\%$ for As) alloys crystallize in a hexagonal crystal structure

 

TABLE I. Experimental volume ($V$) and $c/a$ ratio for $Fe_2P$[29,30] and $Fe_2P_{1-x}T_x$ (T = B, Si, As).[15–17]

| | $V$ (Å$^3$) | $c/a$ |
|---|---|---|
| $Fe_2P$ | 103.10 | 0.589 |
| $Fe_2P_{0.92}B_{0.08}$ | 102.14 | 0.570 |
| $Fe_2P_{0.9}Si_{0.1}$ | 103.92 | 0.578 |
| $Fe_2P_{0.9}As_{0.1}$ | 104.63 | 0.580 |

(space group $P\bar{6}2m$)[29,30] with six Fe atoms and three P atoms per unit cell. There are two inequivalent Fe and P sites. The Fe-I $3f$ (tetrahedral) and the Fe-II $3g$ (pyramidal) sites are triple degenerate, the P-I $2c$ site is double degenerate, and the P-II $1b$ site is nondegenerate. The effect of doping is experimentally known to manifest in a volume ($V$) and $c/a$-ratio change within the hexagonal crystallographic phase (see Table I). Doping beyond the above specified limits leads to crystallographic phase transition/separation (indicated as dashed lines in Fig. 1).

The two internal parameters for $Fe_2P$ in the $P\bar{6}2m$ space group are $x_1 = 0.25683$ for the Fe-I sublattice and $x_2 = 0.59461$ for the Fe-II sublattice.[29] There is no experimental information about how the two internal parameters change with B and Si doping. We performed a test to assess the impact of the internal parameters on the calculated properties. To this end, we used the internal parameters measured for $FeMnP_{0.5}Si_{0.5}$[31] and calculated the exchange interactions ($J_{ij}$) of $Fe_2P$ at its own experimental structure (using the volume and $c/a$ ratio listed in Table I). The obtained effect is less than 1% on the $J_{ij}$'s of $Fe_2P$. Due to the two inequivalent P sites, a preferential site occupance for B and As was found experimentally.[15,17] In the case of Si, site preference was shown so far only by the theoretical calculations.[27,32] The difference between $J_{ij}$'s calculated for the uniformly and preferentially doped $Fe_2P_{1-x}T_x$ at the corresponding experimental structures is about 1%. Therefore, results presented in Sec. III were obtained for uniformly doped P sites and for internal parameters fixed to those measured for $Fe_2P$.

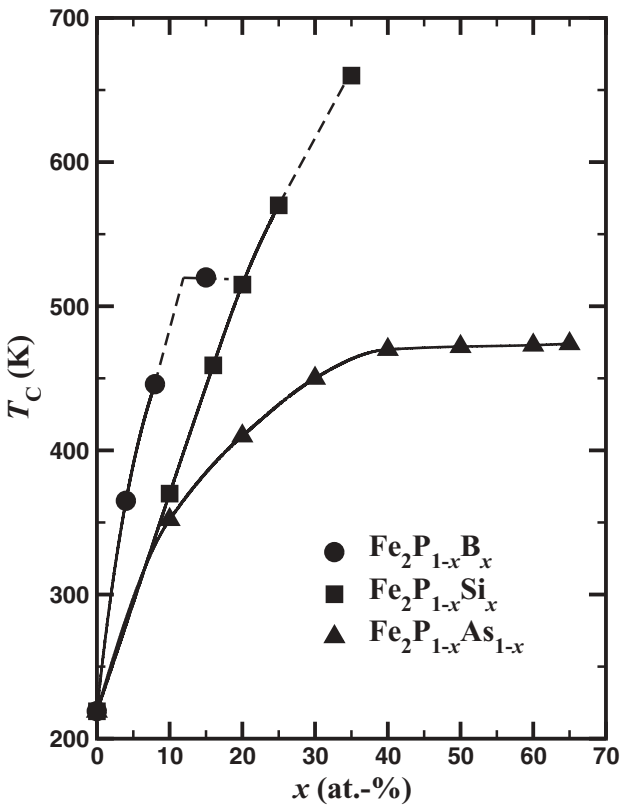


FIG. 1. Experimental Curie temperature ($T_C$) of $Fe_2P_{1-x}T_x$ (T = B, Si, As) as a function of the atomic percentage of dopant element:[15–17] circles represent B; squares, Si; and triangles, As. Dashed lines indicate a crystallographic phase transition for $Fe_2P_{1-x}Si_x$ and phase separation for $Fe_2P_{1-x}B_x$.

The exchange interactions, $J_{ij}$ ($i$ and $j$ denoting Fe positions), were calculated within the magnetic force theorem:[33]

$$J_{ij} = \frac{1}{4\pi}\mathrm{Im}\int_{-\infty}^{E_F} dE\,\mathrm{Tr}_L(\Delta_i T_{ij,\uparrow}\Delta_j T_{ji,\downarrow}), \qquad (1)$$

where $\Delta_i = t_{i,\uparrow}^{-1} - t_{i,\downarrow}^{-1}$ and $t_{i,s}$ and $T_{ij,s}$ ($s = \uparrow, \downarrow$) are the spin-projected single-site scattering matrices and matrices of the scattering path operator, respectively. Note that the trace was taken in angular momentum space, $L = (\ell,m)$, and we omitted labeling explicitly the energy dependence of the occurring scattering matrices. The scattering matrices in turn were obtained using the exact muffin-tin orbital (EMTO) method.[34–37] The EMTO theory formulates an efficient way to solve the Kohn-Sham equation.[38] A full description of the EMTO theory and the corresponding method may be found in Refs. 34–37. Within this approach the compositional disorder was treated using the coherent potential approximation.[39,40]

The one-electron equations were solved within the scalar-relativistic and soft-core approximations. The Green's function was calculated for 20 complex energy points distributed exponentially on an ellipsoidal contour including states within 1.5 Ry below the Fermi level. In the basis set $s$, $p$, and $d$ orbitals were included, and in the one-center expansion of the full charge density a cutoff of $l^h_{\max} = 10$ was used. The electrostatic correction to the single-site coherent-potential approximation was described using the screened impurity model[41] with a screening parameter of 0.902. The Fe $3d$ and $4s$ and the B, As, P, and Si $2/4/3s$ and $2/4/3p$ electrons were treated as valence electrons, respectively. To obtain the accuracy needed for the calculations a $21 \times 21 \times 27$ $k$-point mesh was used within the Monkhorst-Pack scheme. The self-consistent EMTO calculations were performed within the local spin density approximation,[42] which gave a good description of the magnetic properties of $Fe_2P$.[22,23,26,43]

## III. RESULTS

The crystal structure as discussed above implies that the exchange couplings for the pairs of Fe atoms can be cast into six groups. In what follows, Fe atoms in the $3f$ and $3g$ positions are labeled 1–3 and 4–6, respectively. The following exchange coupling parameters are identical due to symmetry relations:

$$J_{11} = J_{22} = J_{33} \equiv \mathbf{J_{11}},$$
$$J_{12} = J_{13} = J_{23} \equiv \mathbf{J_{12}},$$
$$J_{14} = J_{25} = J_{36} \equiv \mathbf{J_{14}},$$

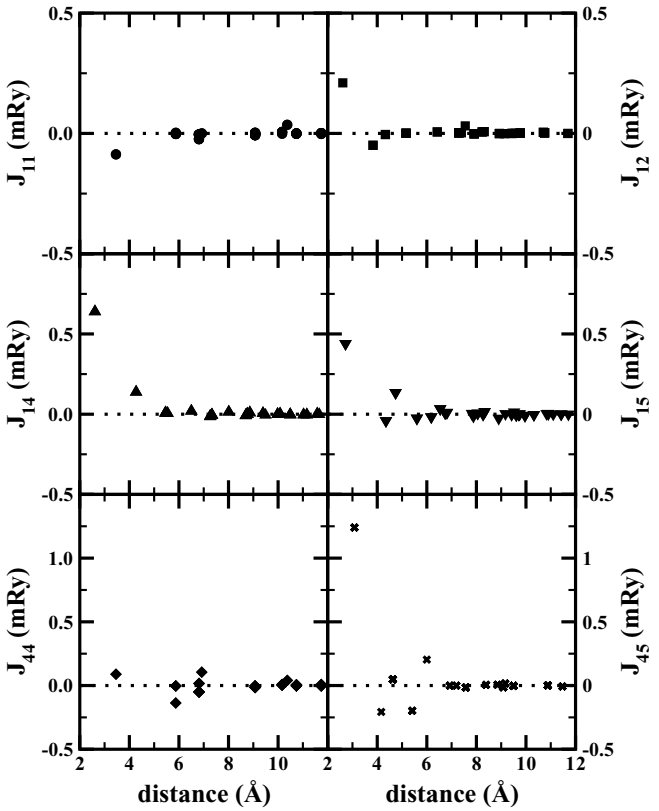


FIG. 2. Calculated Fe-Fe exchange interactions for $Fe_2P$ as a function of distance (in Å). The interactions $\mathbf{J_{ij}}$ are sorted into symmetry-related groups as explained in the text.

$$J_{15} = J_{16} = J_{24} = J_{26} = J_{34} = J_{35} \equiv \mathbf{J_{15}},$$
$$J_{44} = J_{55} = J_{66} \equiv \mathbf{J_{44}},$$
$$J_{45} = J_{46} = J_{56} \equiv \mathbf{J_{45}},$$

where we label the interactions for the groups $\mathbf{J_{ij}}$. Note that, by definition, $J_{ij} = J_{ji}$.

### A. Magnetic interactions of $Fe_2P$

The magnetic interactions of $Fe_2P$ are calculated using the experimental structure parameters (see Table I). The characteristic behavior of the magnetic interactions as a function of the distance is presented in Fig. 2. Note the oscillatory behavior, which falls off with the distance. The strongest interactions turn out to be between the different nearest neighbor Fe-II atoms in the $3g$ position: $\mathbf{J_{45}}$. The next strongest interactions are between Fe-I and Fe-II atoms in the $3f$-$3g$ position, e.g., $\mathbf{J_{14}}$, $\mathbf{J_{15}}$. In addition, we note that the $\mathbf{J_{11}}$ nearest neighbor interactions are actually negative, even though $Fe_2P$ is a FM material. However, these interactions are very weak. In addition, the nearest neighbor $\mathbf{J_{44}}$ interactions are almost 0. Overall, the exchange interactions shown in Fig. 2 are by far the largest for the first few atomic shells, as is typical for metallic, itinerant magnets.

### B. Structural effects on the magnetic interactions of $Fe_2P$

To demonstrate the volume and $c/a$-ratio effect on the individual exchange interactions, we sum up these interactions

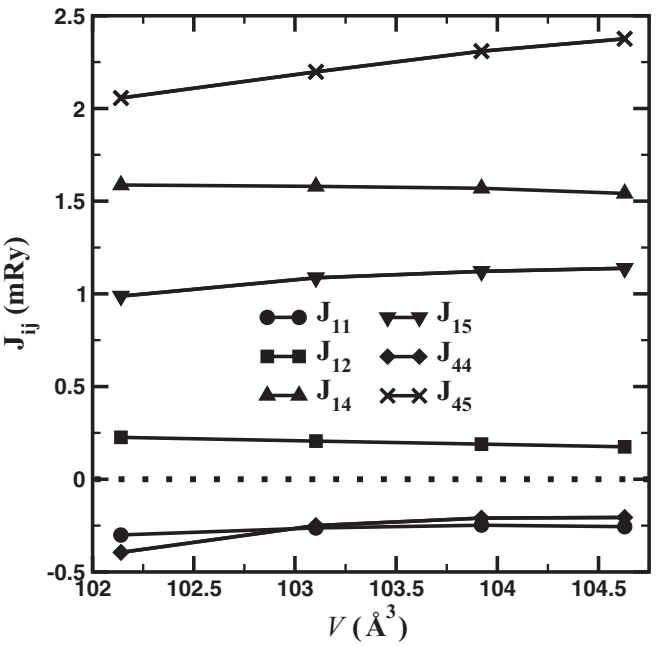


FIG. 3. Accumulated exchange interactions (see text) including the long-range effects for the six groups of Fe-Fe pairs of $Fe_2P$ as a function of volume at the experimental $c/a$ ratio ($c/a = 0.589$).

related to all of the previously introduced classes within a distance of $2a$ (11.735 Å). This involves summing the interaction over 88 shells around each Fe atom. The accumulated interactions include long-range effects and are plotted in Figs. 3 and 4 for $Fe_2P$ as a function of volume and $c/a$ ratio, respectively.

From Figs. 3 and 4, it is obvious that the $\mathbf{J_{ij}}$'s corresponding to groups of Fe-Fe pairs of different symmetry show different (increasing or decreasing) trends as a function of $V$ and $c/a$

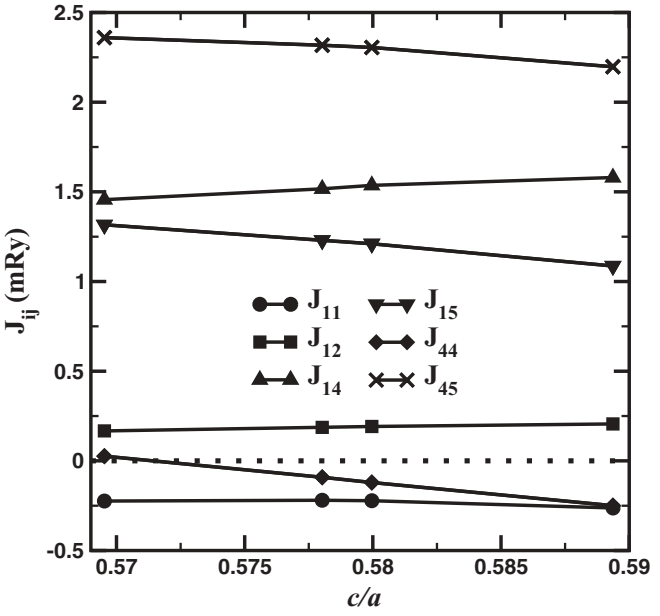


FIG. 4. Accumulated exchange interactions (see text) including the long-range effects for the six groups of Fe-Fe pairs of $Fe_2P$ as a function of $c/a$ ratio at the experimental volume ($V = 103.10$ Å$^3$).

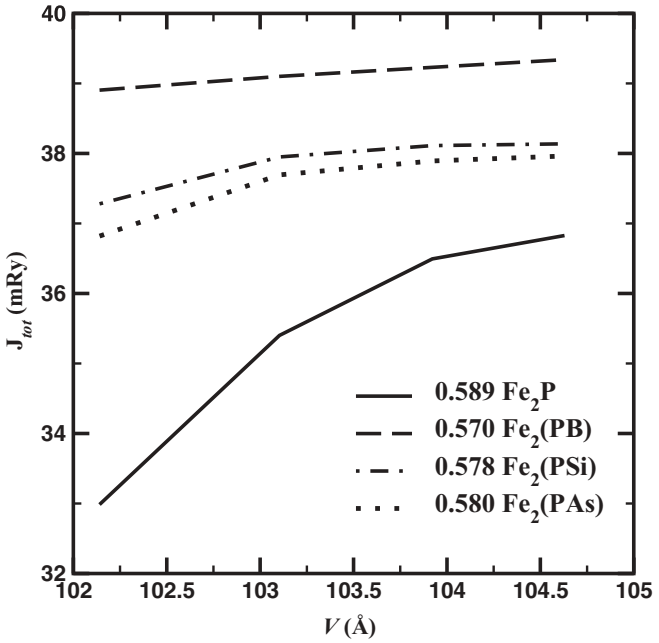


FIG. 5. $\mathbf{J}_{\text{tot}}$ of $Fe_2P$ as a function of volume at different $c/a$ ratios. The $c/a$ ratios correspond to values found experimentally for $Fe_2P$ (solid line), $Fe_2P_{0.92}B_{0.08}$ (dashed line), $Fe_2P_{0.9}Si_{0.1}$ (dashed-dotted line), and $Fe_2P_{0.9}As_{0.1}$ (dotted line).

ratio. On the other hand, two ($\mathbf{J_{45}}$ and $\mathbf{J_{15}}$) of the three largest interactions show similar trends, whereas the third one ($\mathbf{J_{14}}$) has an almost-vanishing volume (Fig. 3) and $c/a$-ratio (Fig. 4) dependence. Based on this observation, we can conclude that the leading exchange interactions increase with increasing volume and decreasing $c/a$ ratio. In order to bring this conclusion to a more quantitative level, we introduce the quantity of the total magnetic exchange interaction ($\mathbf{J}_{\text{tot}}$) as the sum of all the (accumulated) interactions and investigate its behavior as a function of $V$ and $c/a$ ratio. The general trends, shown in Fig. 5, can be summarized as follows: with an increase in the $c/a$ ratio the $\mathbf{J}_{\text{tot}}$ decreases, and with an increase in the volume the $\mathbf{J}_{\text{tot}}$ increases. It is important to point out that $\mathbf{J}_{\text{tot}}$ follows the behavior of the leading terms in Figs. 3 and 4 and thus can be used as a simple representation of the main magnetic interactions.

The above volume effect is in line with the experimental findings, namely, that pressure leads to a decrease in the $T_C$ of $Fe_2P$.[8,44,45] Figure 5 reveals the strong dependence of the exchange coupling parameter with higher $c/a$ ratios, indicating stronger magnetovolume effects for the parent $Fe_2P$ composition.

### C. Chemical and structural contributions to exchange interactions in $Fe_2P_{1-x}T_x$

In the following, we investigate the chemical effect on the magnetic interactions of $Fe_2P$ and the manifested structural effects for three $Fe_2P$-based alloys: $Fe_2P_{0.92}B_{0.08}$, $Fe_2P_{0.9}Si_{0.1}$, and $Fe_2P_{0.9}As_{0.1}$. For the sake of simplicity, in this investigation we focus on $\mathbf{J}_{\text{tot}}$ as an average measure of the leading magnetic interactions. However, we point out that the following conclusions remain valid also if performed on individual (leading) interactions.

TABLE II. Change in the experimental structural parameters ($V$ and $c/a$ ratio, in %) upon doping relative to those of $Fe_2P$ and the theoretical change in $\mathbf{J}_{\text{tot}}$ ($\Delta\mathbf{J}_{\text{tot}}$; mRy) for B-, Si-, and As-doped $Fe_2P$. The total change is decomposed into chemical and structural effects, and in the last two columns we list the two components of the latter one: volume and $c/a$-ratio effects.

| | | | $\Delta\mathbf{J}_{\text{tot}}$ | | | | |
|---|---|---|---|---|---|---|---|
| | $\Delta c/a$ (%) | $\Delta V$ (%) | Total | Chemical | Structural | $c/a$ | $V$ |
| $Fe_2P_{0.92}B_{0.08}$ | −3.37 | −0.93 | 6.70 | 2.23 | 4.46 | 5.96 | −1.49 |
| $Fe_2P_{0.9}Si_{0.1}$ | −1.92 | 0.79 | 4.25 | 0.13 | 4.12 | 2.72 | 1.40 |
| $Fe_2P_{0.9}As_{0.1}$ | −1.60 | 1.48 | 2.73 | −0.05 | 2.78 | 1.15 | 1.63 |

To avoid the superimposition of different contributions (chemical and structural), the chemical effect of doping elements is investigated within the $Fe_2P$ experimental structure. That is, we perform additional calculations for doped systems using the experimental crystal structure of $Fe_2P$. The structural contribution is calculated at a fixed composition by changing the $c/a$ ratio and $V$ according to the experimental changes. Results are listed in Table II.

First, we consider the chemical effects and compare them with the total changes in $\mathbf{J}_{\text{tot}}$. We find that B has the largest chemical effect (33% relative to the total change in $\mathbf{J}_{\text{tot}}$), and this change is positive, i.e., it strengthens the magnetic interactions. For Si and As the chemical effects are found to be minor, 3% and −2%, respectively.

We note that the experimental $c/a$ ratio decreases relative to that of the $Fe_2P$ for all three alloys (see Tables I and II). It is found that $\mathbf{J}_{\text{tot}}$ increases for all alloys as a result of the alloying-induced $c/a$-ratio decrease, in accordance with the trend obtained for $Fe_2P$. The $c/a$-ratio effect represents 88% (64%, 42%) of the total $\Delta\mathbf{J}_{\text{tot}}$ for the B (Si, As)-doped system.

The experimental volume increases relative to that of the $Fe_2P$ for $Fe_2P_{0.9}Si_{0.1}$ and $Fe_2P_{0.9}As_{0.1}$, leading to an increased total magnetic exchange interaction according to the trend obtained for $Fe_2P$. In the case of B-doped $Fe_2P$, the decreased volume leads to a decreased $\mathbf{J}_{\text{tot}}$. The magnitude of the volume change is almost equal, but with opposite sign, for $Fe_2P_{0.92}B_{0.08}$ and $Fe_2P_{0.9}Si_{0.1}$, which is reflected in the $\mathbf{J}_{\text{tot}}$ change. As expected, the volume effect is more accentuated in the case of the As-doped system, for which the $c/a$ ratio is higher than that of the other doped systems. The total structural effect is about 66% (97%, 100%) of the total effect for $Fe_2P_{0.92}B_{0.08}$ ($Fe_2P_{0.9}Si_{0.1}$, $Fe_2P_{0.9}As_{0.1}$).

Summing up the different contributions, we find that the total change in $\mathbf{J}_{\text{tot}}$ is also in line with the experimental findings: B has almost twice as large an effect on the Curie temperature than Si, and As has the smallest effect. However, we should also point out that $\Delta\mathbf{J}_{\text{tot}}$, upon doping with B (Si, As), represents just an 18% (11%, 7%) increase (relative to $Fe_2P$), which is much smaller than the experimental change in $T_C$. The reason for this discrepancy is presently unknown, but it seems to suggest that the present magnetic interactions cannot be used as a direct measure of the magnetic ordering temperature in

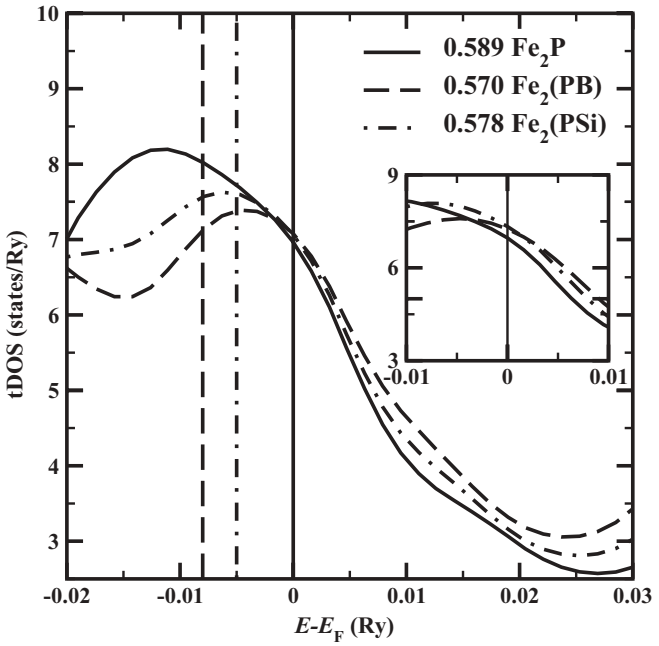


FIG. 6. Total density of states (tDOS) around the Fermi level ($E_F$) of $Fe_2P$ at different $c/a$ ratios, which correspond to the experimental $c/a$-ratio value of $Fe_2P$ (solid line), $Fe_2P_{0.92}B_{0.08}$ (dashed line), and $Fe_2P_{0.9}Si_{0.1}$ (dashed-dotted line). The solid vertical line corresponds to the $E_F$ of $Fe_2P$. The dashed and dashed-dotted vertical lines correspond to the estimated Fermi level of $Fe_2P_{0.92}B_{0.08}$ and $Fe_2P_{0.9}Si_{0.1}$, respectively, using the rigid band model. Inset: tDOS around the $E_F$ of $Fe_2P$ (solid line), $Fe_2P_{0.92}B_{0.08}$ (dashed line), and $Fe_2P_{0.9}Si_{0.1}$ (dashed-dotted line), respectively, calculated at a fixed (0.589) $c/a$ ratio.

$Fe_2P$-based compounds and that other complications in the electronic structure or magnetic interactions come into play.

## IV. DISCUSSION

For $Fe_2P$, $\mathbf{J_{45}}$ values are positive and large (∼1.5 mRy), indicating a strong FM coupling among the Fe-II atoms. However, the exchange interactions between the Fe-I atoms were found to be much smaller (Fig. 2), reflecting their low tendency to order magnetically.

Using the Landau phenomenological theory, Yamada and Terao proposed that the Fe-I sublattice shows a metamagnetic behavior[26] in $Fe_2P$. One consequence of this effect is that in the FM phase, nonzero moments appear in the Fe-I as a result of the exchange field created by the Fe-II atoms. This is indeed reflected by the intermediate positive $\mathbf{J_{14}}$ and $\mathbf{J_{15}}$ interactions between the Fe-I and the Fe-II sublattices shown in the present study. The other consequence is that, near the magnetic transition and in the PM phase, when the exchange field created by the Fe-II atoms vanishes, the magnetic moments in the Fe-I atoms disappear. This is seen in the previous disordered local magnetic moment calculations used to model the PM phase of $Fe_2P$[25,27] and $Fe_2P_{1-x}Si_x$.[27]

Analyzing the change in the exchange coupling parameters attributed to the altered composition, lattice volume, and $c/a$ ratio, respectively, we find that the more robust Fe-II–Fe-II interactions are less affected by these factors than the interlayer (Fe-I–Fe-II) interactions. These findings suggest that the large effect on $T_C$ of doping is connected to how the change in the metamagnetic behavior of the Fe-I site affects the interlayer interactions.

The total change in $\mathbf{J_{15}}$ (4.55, 2.67, and 1.96 mRy for $Fe_2P_{0.92}B_{0.08}$, $Fe_2P_{0.9}Si_{0.1}$, and $Fe_2P_{0.9}As_{0.1}$, respectively) makes the largest contribution (67%, 62%, and 71%, respectively) to the total $\Delta\mathbf{J}_{tot}$. The 98%, 78%, and 65% of the total change in $\mathbf{J_{15}}$ coming from the $c/a$-ratio effect (4.44, 2.07, and 1.27 mRy) for $Fe_2P_{0.92}B_{0.08}$, $Fe_2P_{0.9}Si_{0.1}$, and $Fe_2P_{0.9}As_{0.1}$, respectively. That is, $\Delta\mathbf{J_{15}}$ due to the $c/a$-ratio effect represents 66%, 49%, and 47% of the total $\Delta\mathbf{J}_{tot}$ for $Fe_2P_{0.92}B_{0.08}$, $Fe_2P_{0.9}Si_{0.1}$, and $Fe_2P_{0.9}As_{0.1}$, respectively. For $Fe_2P_{0.9}As_{0.1}$ the effect of the volume change is comparable to the $c/a$-ratio effect on the $\mathbf{J_{15}}$ and strengthens the interlayer $\mathbf{J_{45}}$ interactions.

In order to understand the alloying effect on the structural changes we investigate the density of states (DOS) of $Fe_2P$. Figure 6 shows the total DOS (tDOS) of $Fe_2P$ at different $c/a$ ratios. We find that the $c/a$ ratio has no significant effect on the tDOS at the Fermi level. Within the rigid band model, the Fermi level of the B- and Si-doped systems is shifted toward lower energies as a result of electron removal. The tDOS of $Fe_2P_{0.92}B_{0.08}$ and $Fe_2P_{0.9}Si_{0.1}$ at their estimated Fermi levels (dashed and dashed-dotted vertical lines in Fig. 6) is increased relative to the tDOS of $Fe_2P$. Indeed, the chemical effect of B and Si at a fixed structure of $Fe_2P$ increases the tDOS at the Fermi level (shown in the inset in Fig. 6). On the other hand, in B- and Si-doped systems, the tDOS turns out to be very sensitive to the $c/a$ ratio. Namely, for lower $c/a$ ratios the tDOS is smaller at the estimated $E_F$, i.e., the kinetic energy favors a lower $c/a$ ratio for B- and Si-doped systems. This scenario explains the large $c/a$-ratio drop observed upon doping $Fe_2P$ with B and Si.

## V. CONCLUSION

Using density functional theory formulated within the EMTO method, we have shown that the $c/a$-ratio and volume effects on the leading exchange interactions in alloyed $Fe_2P$ systems obey a general trend: upon increasing the $c/a$ ratio or decreasing the volume, the total magnetic exchange interaction decreases. The largest contribution to the change of the total magnetic exchange interaction is due to the $c/a$-ratio effect on the interlayer (namely, $\mathbf{J_{15}}$) magnetic interaction.

The decrease in the $c/a$ ratio has an electronic structure origin and leads to an approach of the Fe-I and Fe-II sublattices, which has a key role in the strengthening of $\mathbf{J_{15}}$ with alloying. Other interactions are less affected by alloying. Our findings suggest that doping the P sublattice with elements with fewer valence electrons induce a $c/a$-ratio decrease which finally manifests in a $T_C$ increase. This is an important result in searching for new alloying elements which are used to tune the $T_C$ of a given magnetocaloric material.

Taking into account the structural modifications upon doping, we are able to improve our previous predictions for $Fe_2P_{1-x}Si_x$ regarding the composition dependence of $T_C$ based on the total energy differences[27] calculated at a fixed structure. In the present study we show that the structural

effects are important. The decreased $c/a$ ratio strengthens the interlayer Fe-I–Fe-II interactions, which in turn may affect the metamagnetic behavior of the FeI sublattice. However, the peculiar magnetic behavior of the $Fe_2P$-based alloys with the metamagnetic nature of the specific (Fe-I) site only requires further improvement of the current model. An accurate value of $T_C$ cannot be calculated at present using the $J_{ij}$ calculated for a FM state. We suggest that the metamagnetic behavior of the Fe-I sublattice can be considered by applying a constrained disordered local magnetic moment model to the $Fe_2P$-based alloys together with the structural effects. Such studies are under way.

## ACKNOWLEDGMENTS

The European Research Council, Swedish Research Council, Swedish Energy Agency, Swedish Foundation for International Cooperation in Research and Higher Education (STINT), and Hungarian Scientific Research Fund (research projects OTKA 84078 and K77771-IN83114) are acknowledged for financial support. O.E. also acknowledges support from eSSCENCE, STANDUP, ERC (247062-ASD), and the KAW foundation. Calculations were performed on UPPMAX and NSC-Matter resources. E.K.D.-Cz. acknowledges discussions with A. V. Ruban.

*delczeg@kth.se

[1] O. Tegus, E. Brück, K. H. J. Buschow, and F. R. de Boer, Nature **415**, 150 (2002); O. Tegus, E. Brück, L. Zhang, Dagula, K. H. J. Buschow, and F. R. de Boer, Phys. B **319**, 174 (2002); R. Fruchart, Ann. Chim. Fr. **7**, 563 (1982).

[2] E. Brück, O. Tegus, L. Zhang, X. W. Li, F. R. de Boer, and K. H. J. Buschow, J. Alloys Compd. **383**, 32 (2004).

[3] E. Brück, O. Tegus, D. T. Cam Thanh, and K. H. J. Buschow, J. Magn. Magn. Mater. **310**, 2793 (2007).

[4] W. Dagula, O. Tegus, X. W. Li, L. Song, E. Brück, D. T. Cam Thanh, F. R. de Boer, and K. H. J. Buschow, J. Appl. Phys. **99**, 08Q105 (2006).

[5] D. T. CamThanh, E. Brück, N. T. Trung, J. C. P. Klaasse, K. H. J. Buschow, Z. Q. Ou, O. Tegus, and L. Caron, J. Appl. Phys. **103**, 07B318 (2008).

[6] D. Liu, M. Yue, J. Zhang, T. M. McQueen, J. W. Lynn, X. Wang, Y. Chen, J. Li, R. J. Cava, X. Liu, Z. Altounian, and Q. Huang, Phys. Rev. B **79**, 014435 (2009).

[7] R. Wäppling, L. Häggström, T. Ericsson, S. Devanarayanan, E. Karlsson, B. Carlsson, and S. Rundqvist, J. Solid State Chem. **13**, 258 (1975).

[8] H. Fujii, T. Hõkabe, T. Kamigaichi, and T. Okamato, J. Phys. Soc. Jpn. **43**, 41 (1977).

[9] R. Fruchart, A. Roger, and J. P. Senateur, J. Appl. Phys. **40**, 1250 (1969); D. Fruchart, F. Allab, M. Balli, D. Gignoux, E. K. Hlil, A. Koumina, N. Skryabina, J. Tobola, P. Wolfers, and R. Zach, Physica A **358**, 123 (2005).

[10] S. Kumar, S. Chander, A. Krishnamurthy, and B. K. Srivastava, J. Magn. Magn. Mater. **237**, 135 (2001).

[11] H. Fujii, T. Hõkabe, H. Fujiwara, and T. Okamoto, J. Phys. Soc. Jpn. **44**, 96 (1978); S. N. Dolia, A. Krishnamurthy, V. Ghose, and B. K. Srivastava, J. Phys.: Condens. Matter **5**, 451 (1993).

[12] S. N. Dolia, A. Krishnamurthy, and B. K. Srivastava, J. Phys. C **21**, 6005 (1988).

[13] H. Fujii, T. Hokabe, K. Eguchi, H. Fujiwara, and T. Okamoto, J. Phys. Soc. Jpn. **51**, 414 (1982).

[14] R. Zach, J. Tobola, B. Sredniawa, S. Kaprzyk, C. Casado, M. Bacmann, and D. Fruchart, J. All. Comp. **383**, 322 (2004).

[15] R. Chandra, S. Bjarman, T. Ericsson, L. Häggström, C. Wilkinson, and R. Wäppling, J. Solid State Chem. **34**, 389 (1980).

[16] P. Jernberg, A. A. Yousif, L. Häggström, and Y. Andersson, J. Solid State Chem. **53**, 313 (1984).

[17] A. Catalano, R. J. Arnott, and A. Wold, J. Solid State Chem. **7**, 262 (1973).

[18] L. Lundgren, G. Tarmohamed, and O. Beckman, B. Carlsson, and S. Rundqvist, Phys. Scripta **17**, 39 (1978).

[19] N. H. Dung, Z. Q. Ou, L. Caron, L. Zhang, D. T. CamThan, G. A. de Wijs, R. A. de Groot, K. H. J. Buschow, and E. Brück, Adv. Energy Mater. **1**, 1215 (2011); N. H. Dung, L. Zhang, Z. Q. Ou, and E. Brück, Appl. Phys. Lett. **99**, 092511 (2011).

[20] E. P. Wohlfarth, J. Appl. Phys. **50**, 7542 (1979).

[21] T. Moriya and K. Usami, Solid State Commun. **23**, 935 (1977).

[22] S. Ishida, S. Asano, and J. Ishida, J. Phys. F **17**, 475 (1987).

[23] O. Eriksson, J. Sjöström, B. Johansson, L. Häggström, and H. L. Skriver, J. Magn. Magn. Mater. **74**, 347 (1988).

[24] J. Tobola, M. Bacmann, D. Fruchart, S. Kaprzyk, A. Koumina, S. Niziol, J.-L. Soubeyroux, P. Wolfers, and R. Zach, J. Magn. Magn. Mater. **157–158**, 708 (1996).

[25] B. Wiendlocha, J. Tobola, S. Kaprzyk, R. Zach, E. K. Hlil, and D. Fruchart, J. Phys. D **41**, 205007 (2008).

[26] H. Yamada and K. Terao, Phase Transit. **75**, 131 (2002).

[27] E. K. Delczeg-Czirjak, L. Delczeg, M. P. J. Punkkinen, B. Johansson, O. Eriksson, and L. Vitos, Phys. Rev. B **82**, 085103 (2010).

[28] Z. Gercsi and K. G. Sandeman, Phys. Rev. B **81**, 224426 (2010).

[29] B. Carlsson, M. Gölin, and S. Rundqvist, J. Solid State Chem. **8**, 57–67 (1973).

[30] H. Fujii, S. Komura, T. Takeda, T. Okamoto, Y. Ito, and J. Akamitsu, J. Phys. Soc. Jpn. **46**, 1616 (1979).

[31] V. Höglin, M. Hudl, M. Sahlberg, P. Nordblad, P. Beran, and Y. Andersson, J. Solid State Chem. **184**, 2434 (2011).

[32] X. B. Liu and Z. Altounian, J. Appl. Phys. **105**, 07A902 (2009).

[33] A. I. Liechtenstein, M. I. Katsnelson, and V. A. Gubanov, J. Phys. F **14**, L125 (1984).

[34] O. K. Andersen, O. Jepsen, and G. Krier, in *Lectures on Methods of Electronic Structure Calculation* (World Scientific, Singapore, 1994), p. 63.

[35] L. Vitos, H. L. Skriver, B. Johansson, and J. Kollár, Comp. Mater. Sci. **18**, 24 (2000).

[36] L. Vitos, Phys. Rev. B **64**, 014107 (2001).

[37] L. Vitos, I. A. Abrikosov, and B. Johansson, Phys. Rev. Lett. **87**, 156401 (2001).

[38]W. Kohn and L. J. Sham, Phys. Rev. **140**, A1133 (1965).
[39]P. Soven, Phys. Rev. **156**, 809 (1967).
[40]B. L. Gyorffy, Phys. Rev. B **5**, 2382 (1972).
[41]P. A. Korzhavyi, A. V. Ruban, I. A. Abrikosov, and H. L. Skriver, Phys. Rev. B **51**, 5773 (1995).
[42]J. P. Perdew and Y. Wang, Phys. Rev. B **45**, 13244 (1992).
[43]L. Severin, L. Häggström, L. Nordström, Y. Andersson, and B. Johansson, J. Phys.: Condens. Matter **7**, 185 (1995).
[44]H. Fujiwara, H. Kadomatsu, K. Tohma, H. Fujii, and T. Okamoto, J. Magn. Magn. Mater. **21**, 262 (1980).
[45]H. Kadomatsu, M. Isoda, K. Tohma, H. Fujii, T. Okamoto, and H. Fujiwara, J. Phys. Soc. Jpn. **54**, 2690 (1985).